Exclusive quasi-deuteron absorption of pions in ^{16}O and ^{18}O at 116 MeV

R. A. Schumacher,* P. A. Amaudruz, C. H. Q. Ingram, and U. Sennhauser
Paul Scherrer Institute,† CH-5234 Villigen, Switzerland

H. Breuer, N. S. Chant, A. E. Feldman, B. S. Flanders, F. Khazaie,‡ D. J. Mack,§
P. G. Roos, and J. D. Silk**
University of Maryland, College Park, Maryland 20742

G. S. Kyle
New Mexico State University, Las Cruces, New Mexico 88003
(Received 27 May 1988)

The reaction $^{16}O(\pi^+,2p)^{14}N$ was measured at $T_\pi = 116$ MeV with an excitation energy resolution between 1.6 and 2.5 MeV with one proton angle fixed at 50° and for a wide range of the second angle. Proton angular correlations, energy sharing distributions, and recoil momentum distributions for four strongly populated states are consistent with a model of pion absorption on quasi-deuteron pairs with angular momentum transfer to the recoil nucleus of $L = 0$ (3.9 MeV state), $L = 2$ (7.0 and 11.0 MeV states), or a mixture of $L = 0$ and $L = 2$ (ground state). Integration of the measured absorption cross section over angle and up to 20 MeV of excitation shows that 19±4% of the total absorption cross section can be found in two-proton final states near quasifree kinematics, with substantial additional two-nucleon strength between 20 and roughly 50 MeV of excitation. With estimated corrections for final-state interactions, about half of the absorption cross section below 20 MeV excitation proceeds via the direct quasifree $\pi pn \rightarrow pp$ process. Absorption leading to the $T = 1$ state at 2.3 MeV is $< 5\%$ as strong as absorption to the $T = 0$ ground state. The $^{18}O(\pi^+,2p)^{16}N$ reaction was measured under the same kinematic conditions. States of less than 0.4 MeV excitation, which correspond to absorption on nucleons in different shells, account for at least 6.1±0.6% of the estimated two-nucleon absorption cross section below 20 MeV excitation; no unexpected suppression of cross-shell absorption was found.

I. INTRODUCTION

The aim of this experiment is to improve our understanding of the two-nucleon absorption mechanism in a kinematically complete measurement of the reactions $^{16}O(\pi^+,2p)^{14}N$ and $^{18}O(\pi^+,2p)^{16}N$ at $T_\pi = 116$ MeV. With an energy resolution good enough to separate events leading to individual final states of known structure we can compare with dynamical models which depend upon the quantum numbers of the nucleons involved in the absorption process, and hence test our understanding of the two-body mechanism. In particular, we will show the importance of considering absorption of pions on p-shell pairs with angular momentum $L = 2$ in addition to $L = 0$ with respect to the spectator nucleons.

Quasifree absorption of pions on nucleon pairs with the quantum numbers of the deuteron is an important, perhaps dominant dynamical process for pion absorption in nuclei at energies near the $\Delta(1232)$ resonance.[1,2] It is the only reaction mechanism which has been clearly identified experimentally, but its magnitude is still controversial. The proton spectra from $\pi^+ + A \rightarrow 2p + (A-2)$ measurements show a clear component with kinematics and angular distributions consistent with those of a quasifree, Fermi-broadened $\pi d \rightarrow 2p$ reaction.[3-5] This component is then often identified as the yield from the pion being directly absorbed on two nucleons. Attempts have been made to deduce the full two-nucleon absorption cross section from the direct two-nucleon absorption yield by estimating the losses from initial- and final-state interactions in the latter. The resultant yield may be compared with the total absorption cross section and any deficiency taken as evidence for other reaction dynamics. However, it is experimentally not possible to unambiguously distinguish all reactions with an initial- or final-state interaction—for example those involving small momentum and energy transfer. This ambiguity adds to the uncertainty of the appropriate correction to be applied to the extracted "direct" two-nucleon absorption cross section to obtain the full yield due to two-nucleon dynamics.

One recently used method for experimentally separating direct two-nucleon absorption from the rest is to decompose proton angular correlations into the sum of two Gaussians, where one is "narrow" and near the quasifree kinematics, while the other is "wide" and spreading far from the quasifree kinematics. Equating two-nucleon absorption with the narrow component of the $(\pi,2p)$ angular correlation, Altman *et al.* found about 10% of the total absorption cross section in ^{12}C at resonance.[3] This suggested that even after making corrections for initial- and final-state interactions a large fraction of the absorption cross section is to be found in other, so far unidentified, absorption channels. In a

kinematically complete experiment measuring ^{58}Ni$(\pi,2p)$ at 160 MeV with moderate energy resolution, Burger *et al.* found less than 50% of the absorption cross section in the two-proton channel after estimating initial- and final-state interaction effects.[4] The interpretations of the above-mentioned experimental studies have been disputed, however. Ritchie *et al.*,[6] using calculations of two-nucleon absorption in the distorted-wave impulse approximation (DWIA),[7] concluded that the quasi-deuteron component of the ^{12}C$(\pi^+,2p)$ reaction could have substantial broad components in the two-nucleon angular correlations which might have been excluded in the analysis of Altman *et al.* The model of Refs. 6 and 7 will be discussed below in the context of the present experiment. Gibbs and Kaufmann interpreted the data on ^{58}Ni with an intranuclear cascade calculation and concluded that as much as 70% of the absorption cross section can be explained using only two-body processes.[8]

Other experiments have established that pion absorption often leads to complex final states involving many energetic nucleons,[5,9–11] but our understanding of how these states arise is quite poor. The observation of a $30\pm10\%$ phase-space-like component of three-nucleon absorption in ^{3}He at 120 MeV has suggested that multinucleon mechanisms are important.[12] However, these results are difficult to interpret in the absence of any dynamical signature of a three-body absorption mechanism. Also, the suggestion based on analysis of inclusive (π,p) data that multinucleon absorption might be important has been questioned by Girija and Koltun.[13] Thus the strength of the two-nucleon absorption mechanism in nuclei, and the nature of any others that exist, are still open issues.

This experiment has sufficient energy resolution to resolve individual final states and establishes the importance of absorption on $L=2$ pairs, as postulated by Ritchie *et al.* The shape of the two-proton angular correlation as a function of excitation energy, and its implication for the magnitude of the two-nucleon absorption mechanism is explored.

II. THEORY

The four states strongly excited in the ^{16}O$(\pi^+,2p)^{14}$N reaction are listed together with their dominant shell-model components in Table I. All are $T=0$ states, populated by absorption on pn pairs, and are the same four states strongly excited in the two-nucleon transfer (d,α) reaction.[14] In identifying the quasi-deuteron component of the shell-model configurations, the total spin **J** of two protons $\mathbf{j}_1$ and $\mathbf{j}_2$ is written $\mathbf{J}=\mathbf{j}_1+\mathbf{j}_2=\mathbf{L}+\mathbf{S}$, where $\mathbf{S}=\boldsymbol{l}+\mathbf{s}$ and the relative coordinates are taken to be $l=0$ and $s=1$, as for the $^3S_1$ $T=0$ deuteron. We take $S=1$, so the allowed L values then follow, where odd values are ruled out by the positive parity of the states. The spectroscopic strengths in Table I are two-particle spectroscopic factors given by Cohen and Kurath.[15]

In a spectator model, absorption on an $L=0$ quasi-deuteron is characterized by nucleon angular correlations peaked at quasifree angle pairs, and, at these angle pairs, by energy spectra peaked at corresponding quasifree energies. $L=2$ absorption is characterized by minima at the quasifree angles and energies, with a maximum in angle in a cone surrounding the quasifree angle, and two maxima at energies above and below the quasifree energy. It is these behaviors for which we show experimental evidence.

The experimental data for transitions to specific nuclear states have been compared to factorized DWIA calculations based on a quasideuteron model. Following the work of Roos *et al.*,[7] the triple differential cross section for $A(\pi^+,2p)B$ to a specific final state with angular momentum transfer L in nucleus B is written as

$$\frac{d^3\sigma}{d\Omega_1 d\Omega_2 dE_1}=\mathrm{KF}\frac{d\sigma}{d\Omega}\sum_{\Lambda}|T_{BA}^{L\Lambda}|^2 \tag{1}$$

with

$$T_{BA}^{L\Lambda}=\frac{1}{(2L+1)^{1/2}}\int \chi_{p1B}^{(-)*}(\mathbf{k}_{p1B},\mathbf{r})\chi_{p2B}^{(-)*}(\mathbf{k}_{p2B},\mathbf{r}) \times\chi_{\pi A}^{(+)}\left(\mathbf{k}_{\pi A},\frac{B}{A}\mathbf{r}\right)\phi_{L\Lambda}(\mathbf{r})d^3r\ . \tag{2}$$

In Eq. (1) the quantity KF represents a known kinematic factor and $d\sigma/d\Omega$ represents the off-shell πNN vertex. In the present calculations we have assumed a particular prescription which takes $d\sigma/d\Omega$ to be equal to the on-shell (experimental) $\pi^+ + d\rightarrow 2p$ cross section. The effective $\pi^+ + d\rightarrow 2p$ angle and energy were determined from the outgoing proton momenta; the strong dependence of this cross section on angle and energy produces

TABLE I. Principal $T=0$ states excited in the reaction ^{16}O$(\pi^+,2p)^{14}$N and their dominant shell-model components (Ref. 15), plus the $T=1$ state at 2.31 MeV which may be weakly populated in this reaction.

E_x (MeV)	J^π	T	Configuration	Spectroscopic factors for states with (T,L): (0,0)	(0,2)	(1,0)
0	1^+	0	$(p_{1/2})^{-2}$	0.016	2.704	
2.313	0^+	1	$(p_{1/2})^{-2}$			2.212
3.948	1^+	0	$(p_{3/2}^{-1},p_{1/2}^{-1})$	2.675	0.081	
7.028	2^+	0	$(p_{3/2}^{-1},p_{1/2}^{-1})$		5.0	
11.05	3^+	0	$(p_{3/2})^{-2}$		7.0	

significant effects in both the energy sharing and angular distributions.

In the amplitude $T_{BA}^{L\Lambda}$ [Eq. (2)] the χ's represent distorted waves calculated with optical-model potentials obtained from fits to elastic scattering data. For the $\pi^+ - {}^{16}O$ optical-model potential we have used a Kisslinger-type potential with parameters obtained from an energy-dependent analysis of $\pi^+ - {}^{12}C$ scattering by Amann *et al.*[16] The $p - {}^{14}N$ optical-model potentials were taken from the global analysis of intermediate energy proton elastic scattering by Nadasen *et al.*[17]

A major ingredient in the calculation of the amplitude $T_{BA}^{L\Lambda}$ is the coordinate space wave function for the center-of-mass motion of the pair represented by $\phi_{L\Lambda}(r)$ where Λ is the projection of the orbital angular momentum L. To generate $\phi_{L\Lambda}(r)$ we have employed the techniques developed for the generation of microscopic form factors for two-nucleon transfer DWBA calculations. We have used the p-shell wave functions of Cohen and Kurath[15] to describe the states in ^{14}N, assuming a closed-shell ^{16}O target nucleus. The p-shell single-particle wave functions were calculated for a Woods-Saxon potential with the geometrical parameters taken from the work of Elton and Swift[18] and with a well depth chosen to reproduce one-half of the neutron-proton separation energy. In the present calculations of the form factors $\phi_{L\Lambda}(r)$ the two-particle wave functions resulting from the overlap of the closed-shell ^{16}O with the two-hole ^{14}N wave functions were recoupled to total orbital angular momentum L and total spin S, and then transformed numerically to the relative and center-of-mass coordinates of the pair. Finally an overlap of the resultant with a Hulthen deuteron wave function was taken. Thus, in our calculations presented in the next section, $\phi_{L\Lambda}(r)$ represents the motion of the center of mass of a np pair with both the internal quantum numbers ($l=0$, $s=1$, $t=0$) and the relative motion wave function of a physical deuteron and contains the spectroscopic amplitude predicted by the Cohen-Kurath shell-model wave functions.

Before discussing the experimental results it is important to note several simplifying approximations of the present calculations. First, the expression given in Eq. (1), in which the unpolarized $\pi^+ + d \rightarrow 2p$ cross section enters as a multiplicative factor, is correct only for $L=0$. More correctly, the factorized DWIA expression involves a summation in which different values of L, Λ, and different deuteron spin projections enter coherently. As pointed out by Gouweloos and Thies,[19] for $L>0$ this is equivalent to an effective tensor polarization of the struck deuteron and thus necessitates a more detailed treatment of the $\pi^+ + d \rightarrow 2p$ spin amplitudes. Modelling these by assuming dominance of the s-wave Δ-nucleon term (i.e., following Ref. 19 and retaining only their A_5 term) our major conclusions are unchanged.[20] Fortunately, the possible coherence between $L=0$ and $L=2$ terms should not play a major role in the calculations for the 1^+ transitions. Specifically, the Cohen-Kurath wave functions are dominated by the $L=0$ term for the 3.9 MeV 1^+ state and by the $L=2$ term for the ground state 1^+ transition. Furthermore, at the low recoil momenta where $L=0$ amplitudes are large, $L=2$ amplitudes should be small. Nevertheless, since the $L=0$ contribution does appear to be significant for the ground-state transition, more detailed calculations are of interest. Second, in the present calculations, the two-nucleon wave functions are projected onto a "physical" (i.e., Hulthen) deuteron. Restriction of the pn pair to the $S=1$ and $T=0$ quantum numbers is probably reasonable based on experimental evidence that capture on the "singlet" pair is very small.[21,22] The restriction to $l=0$ for the relative np motion is more questionable, but calculations by Ohta, Thies, and Lee suggest that the $l\neq 0$ terms are $<20\%$. Use of the relatively long-ranged "physical" deuteron radial wave function leads to a relatively long-ranged two-nucleon absorption mechanism. Gouweloos and Thies prefer to use a shorter range (of ~ 1 fm), which leads to a significant enhancement of the cross section (>2) over what is obtained with the longer ranged interaction. We will return to this point in the comparison of the calculations with the experimental data. In spite of the above concerns we will see that the calculations provide useful insight into the importance of distortions, the energy and angle dependence of the elementary $\pi^+ + d \rightarrow 2p$ amplitude, and the effect of absorbing on $L>0$ pairs.

III. EXPERIMENTAL PROCEDURE AND DATA ANALYSIS

The layout of the experimental apparatus is shown in Fig. 1. In the following discussion we use the coordinate system $(\hat{x},\hat{y},\hat{z})$, where $\hat{z}$ is the beam direction, $(\hat{x},\hat{z})$ defines the beam-spectrometer scattering plane, and the in-plane scattering angle θ of a particle momentum vec-

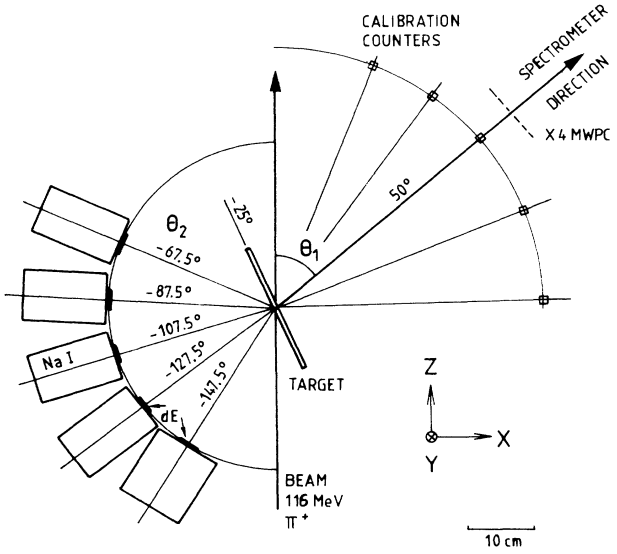

FIG. 1. Layout of the experiment at the SIN $\pi M1$ channel showing incident pion beam, $^1H_2O/^2H_2O$ target, SUSI spectrometer position, and positions of the in-plane NaI detectors. Four additional elements of the NaI array were mounted $\beta=20°$ above the plane. Calibration counters (scintillator fingers) were used to monitor the gain stability of the NaI detectors via the $^2H(\pi^+,2p)$ reaction.

tor $\mathbf{p}$ is $\cos^{-1}(\hat{\mathbf{p}}_{xz}\cdot\hat{\mathbf{z}})$. The out-of-plane angle β is defined as $\tan^{-1}(-p_y/|p_{xz}|)$, which is the angle out of the $(\hat{\mathbf{x}},\hat{\mathbf{z}})$ plane.

A 116-MeV position pion beam of typically 5×10^6/sec from the $\pi M1$ channel at the Swiss Institute for Nuclear Research[23] (SIN) was incident on a thin water target. The first nucleon p_1 was detected at $\theta_1=+50°$ with respect to the beam in the energy range 60 MeV $< T_1 <$ 175 MeV with the SUSI magnetic spectrometer.[23] The second nucleon p_2 was detected in a five-element array of NaI detectors covering the angular range $\theta_2=-57.5°$ to $-147.5°$ in 10° steps (in two angle settings) in the energy range 30 MeV $< T_2 <$ 200 MeV. A second arc of four NaI detectors at $\beta=20°$ covered the range $\theta_2=-77.5°$ to $-147.5°$. Scintillator trigger counters in front of the NaI detectors defined a solid angle of 19.2 msr for each element of the array. The spectrometer solid angle was about 14 msr, and the actual combination of solid angle and target thickness was determined by normalization to known $^{16}O(\pi^+,\pi^+)$,$^1H(\pi^+,\pi^+)$, and $^2H(\pi^+,2p)$ cross sections. The target contained 10% by volume deuterated water, making possible an energy calibration of the NaI detectors simultaneous with the oxygen data taking. For this purpose, scintillation detectors labeled "calibration counters" in Fig. 1 were placed at the angles conjugate to the NaI detectors for the $^2H(\pi^+,2p)$ reaction.

A. Experimental details

The momentum spread of the pion beam was $\delta p/p=4\%$, but the momentum of each pion was determined to within 0.25% by an in-beam hodoscope placed at the momentum-dispersed focus at the midpoint of the channel. A 1-mm-thick scintillator placed 50 cm upstream of the target detected each incident pion. Pions were separated from muons and electrons by time of flight over the 20-m path length from the production target. Protons were largely eliminated by an electrostatic separator in the beam, with any residual contamination eliminated by time of flight and scintillator pulse-height analysis. The target was placed at $-25°$ with respect to the beam, the angle at which energy losses among the pions and protons were best matched and contributed less than 0.5 MeV to the excitation energy resolution under quasifree kinematics. The beam spot in the target plane, as imaged by the multiwire proportional chambers (MWPC's) at the spectrometer entrance, was 29×10 mm^2 FWHM (horizontal $\times$ vertical), with an angular spread (unmeasured) of ±30 mrad horizontally and ±62 mrad vertically.

The water targets were nominally 100 mg/cm^2 thick, constructed using walls of stretched, 5-μm-thick titanium. Micrometer-thickness measurements of the filled targets determined the actual average thickness to within ±10 mg/cm^2, and periodic weighing assured that the targets were watertight. A helium bag surrounded the target to reduce background. Runs with an empty target were performed and showed that the only significant background contribution from the target was isolated at about -6 MeV of excitation with respect to the oxygen ground state (see Fig. 9); these events originated from the titanium foils.

The SUSI magnetic spectrometer was used in a standard two-quadrupole configuration. The data were obtained in two nonoverlapping momentum settings, the first centered at 377 MeV/c which covered the proton energies 60 to 100 MeV, and the second centered at 510 MeV/c which covered the proton energies 100–175 MeV. The allowed time-of-flight window through the spectrometer assured that all triggering particles were protons. A parameterization taken from previous work corrected the spectrometer acceptance roll off as a function of $\delta p/p$.[11] The acceptance was truncated when this correction reached a factor of 2; for the central 80% of the acceptance range the correction did not exceed 20%. The combined efficiency of the six MWPC planes in the spectrometer was typically 75%.

The NaI detectors were of two types. Seven detectors were Harshaw Integral Line Units ($7.6\times7.6\times12.7$ cm^3), capable of stopping up to 210-MeV protons. The largest angle detector in the array was a Bicron device ($10.2\times10.2\times17.8$ cm^3) placed such that it simultaneously filled both an in-plane ($\beta=0°$) and an out-of-plane ($\beta=20°$) position in the NaI array as defined by two separate dE counters. The scintillator trigger counters were $3.0\times4.0\times0.2$ cm^3 and were 25 cm from the target center. Their size was such that protons of up to 200 MeV originating from any point within the target spot would stop in the NaI detectors. The energy resolution of the detectors was typically 1% for 100-MeV protons.

Gain stabilization and calibration of the phototubes was important to compensate the effects of gain changes on the scale of minutes caused by changes in the beam intensity, and diurnal gain changes caused by ambient temperature fluctuation. Gain changes of several percent occurred in response to counting rate changes between 0 and 5 kHz. To stabilize the load on a phototube, a light-emitting diode mounted next to the phototube face flashed at rates varying with the particle rates to maintain a steady total rate of typically 5 kHz, independent of beam conditions. The pulses from these "background" LED's were adjusted to match those of typical particle pulses. A second LED was used to monitor pulse-height changes by recording LED "events" once per second. Rapid transient gain changes detected by the analysis program switched off the detector until it returned to stability.

Long-term gain changes, particularly those due to daily temperature fluctuations of about 5 °C were monitored and corrected by measuring the energy of protons from the $^2H(\pi^+,2p)$ reaction. Scintillation counters ($1.2\times10.0\times0.5$ cm^3) were placed 40 cm from the target at angles kinematically conjugate to each of the NaI detectors. Coincidences between these calibration counters and NaI detectors represented about one-half of all events recorded. After applying off-line particle identification cuts, peaks in the NaI energy spectra were fitted for data accumulated in time intervals of between 4 and 8 h. Improvements in excitation energy resolution achieved by this method were up to 0.5 MeV FWHM.

B. Data analysis

The data analysis proceeded in two passes, the first to remove the time dependence of the NaI detector energy calibrations as discussed above, and the second to accumulate the angular correlation, energy sharing, and recoil momentum spectra of interest. The spectrometer momentum calibration was taken from previous work.[23] The NaI calibrations were adjusted to optimize the energy resolution for events selected from the ^{14}N ground state. Events were corrected for the energy losses computed for the NaI trigger counters, the target, the helium gas, and various inactive layers of material.

The cross sections were computed according to the expression

$$\frac{d^3\sigma}{d\Omega_1 d\Omega_2 dE_1} = \frac{N_p}{N_\pi} \frac{1}{(\rho t)\Delta\Omega_1\Delta\Omega_2\Delta E_1} \frac{A}{N_0\eta} , \quad (3)$$

where N_p and N_π are the numbers of p-p coincidences and the number of incident pions, respectively, N_0 is Avogadro's number, A the molecular weight of the target, ρt the target thickness, η represents all efficiency and deadtime corrections, and ΔE_1 is the energy bin size. $\Delta\Omega_1\Delta\Omega_2$ is the product of the geometrical solid angles corrected for target spot size effects, which is strictly appropriate only for completely uncorrelated protons. The model calculations discussed in this paper take this into account. In practice, the quantity $\rho t\Delta\Omega_1$ was adjusted such that the absolute ^{16}O and ^{18}O cross sections were normalized to the available single-arm calibration cross sections: ^{16}O(π^+,π^+) (Ref. 24) and ^{1}H(π^+,π^+) (Ref. 25) elastic scattering and ^{2}H(π^+,p) (Ref. 26). The ratio of ^{2}H(π,p) yields in the calibration counters also served to calibrate the relative target thicknesses; the target thickness ratio was found to be $T(^{16}\text{O})/T(^{18}\text{O})=1.052\pm0.045$. Based on a weighted average of factors required to match the above calibration cross sections, the systematic absolute normalization uncertainty was estimated to be $\pm10\%$.

The excitation energy E_x determines the state of the residual nucleus and is defined by $E_x=\sqrt{E_R^2-p_R^2}-M_R$, where

$$E_R=E_\pi+M_T-(E_1+E_2), \quad \mathbf{p}_R=\mathbf{p}_\pi-(\mathbf{p}_1+\mathbf{p}_2)$$

and where M_T and M_R are the target and recoil nucleus masses. Figure 2(a) shows the ^{14}N excitation spectrum for the quasifree angle pair $(\theta_1,\theta_2)=(50°,-107.5°)$, and Fig. 2(b) shows the corresponding spectrum for the pair 20° off quasifree at $(50°,-127.5°)$ but still in the beam-spectrometer ($\beta=0$) plane. The resolution achieved was 1.6 to 2.5 MeV FWHM depending on the detector pair. The numbers of counts in Figs. 2(a) and 2(b) are relatively normalized. One can see that the 3.9 MeV 1^+, $L=0$ state dominates the spectrum at quasifree angles and drops rapidly with angle, while the 0 MeV 1^+ and 7.0 MeV 2^+ $L=2$ states appear roughly unchanged. The number of counts in each peak was extracted with fits to these spectra allowing the relative magnitude and the common width of the main peaks to vary. A continuum background starting at 7.6 MeV was included in the fits as well as unresolved small-amplitude peaks near the energies where there are other states weakly excited in (d,α) scattering. A Gaussian line shape was used to fit the states, and a definition of χ^2 compatible with Poisson statistics was used to properly fit states with small numbers of counts.[27] The stability of the fits was tested by varying the initial conditions and the number of degrees of freedom. The fits to these E_x spectra were used for extracting the angular correlation and recoil momentum results.

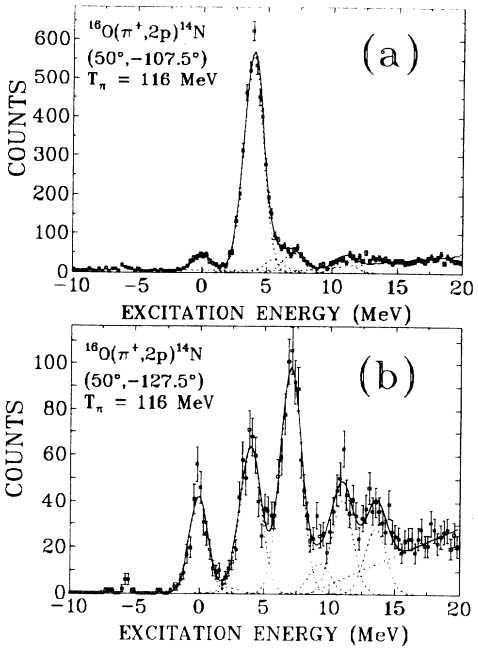

FIG. 2. Excitation energy spectra for the quasifree angle pair (a), and for 20° off quasifree (b). The 3.9 MeV $L=0$ state dominates at the central quasifree angle, while at other angles the $L=2$ states at 0.0, 7.0, and 11.0 MeV are more prominent. Dotted lines show fits used to determine the numbers of events in each state.

Two additional corrections to the data were made. The spectrometer acceptance correction was mentioned above. Reaction losses in the NaI detectors were corrected for by assuming that reactions took events out of the low-lying excitation region, and varied between 3.5 and 7% depending on the average proton energy in each detector.[28] The size of the target spot in relation to the proximity and size of the detection apertures resulted in a geometrical solid angle which varied with event origin. Numerical integration of the solid angles averaged over the target spot showed that the corrections to the point-target solid angle of 19.2 msr were less than $\pm0.5\%$.

IV. RESULTS AND DISCUSSION OF THE ^{16}O$(\pi^+,2p)^{14}$N REACTION

A. Angular correlations of the low-lying $T=0$ states of ^{14}N

The measured angular correlations for protons emitted in the reaction ^{16}O$(\pi^+,2p)^{14}$N leading to the strong $T=0$

states listed in Table I are shown in Fig. 3. These double differential cross sections, $d^2\sigma/d\Omega_1 d\Omega_2$, were obtained after integrating over the proton energy range 60 MeV $< T_1 <$ 175 MeV on the spectrometer side with limits 30 MeV $< T_2 <$ 200 MeV on the NaI array side. The error bars are a combination of statistical errors and estimated errors from the peak-fitting procedure. The circular data points are from the array of detectors in the beam-spectrometer plane ($\beta=0°$), while the triangular points are from the detectors placed at $\beta=20°$ above this plane. The vertical dotted lines indicate the quasifree angle for $\beta=0°$. It is roughly at this same angle that the recoil momentum is minimum for $\beta=20°$. The dashed curve in the ground-state case is discussed below. The solid curves are predictions of the factorized DWIA quasi-deuteron model calculation discussed above, normalized to the data of each state separately. The dot-dashed curves are PWIA versions of the same theory, likewise normalized to the data. The necessary renormalizations of the calculation for the ground, 3.9, 7.0, and 11.0 MeV states are 2.3, 7.0, 4.4, and 1.8 in the DWIA case, and 0.4, 1.7, 0.7, and 0.3 in the PWIA case, respectively. The proton energy acceptance of the apparatus included all but a few percent of the energy phase space for these states, as will be seen in Sec. IV B; no corrections have been made to the data in Fig. 3 for the apparatus' energy acceptance.

The 3.9 MeV $L=0$ state angular correlation peaks at the quasifree angle as expected for absorption on a *pn* pair with a momentum wave function peaked at zero. The width predicted by the factorized quasi-deuteron model calculation is somewhat too narrow, as emphasized by the out-of-plane $\beta=20°$ results. In contrast, the 7.0 MeV $L=2$ state angular correlation is broader and has a peak at about $-125°$, well away from the quasifree angle. The same behavior is seen in the $L=2$ state at 11 MeV, even though the point-to-point errors are larger here owing to the uncertainties of fitting this state in the continuum background. The observed single peak at backward angle, rather than the expected double-

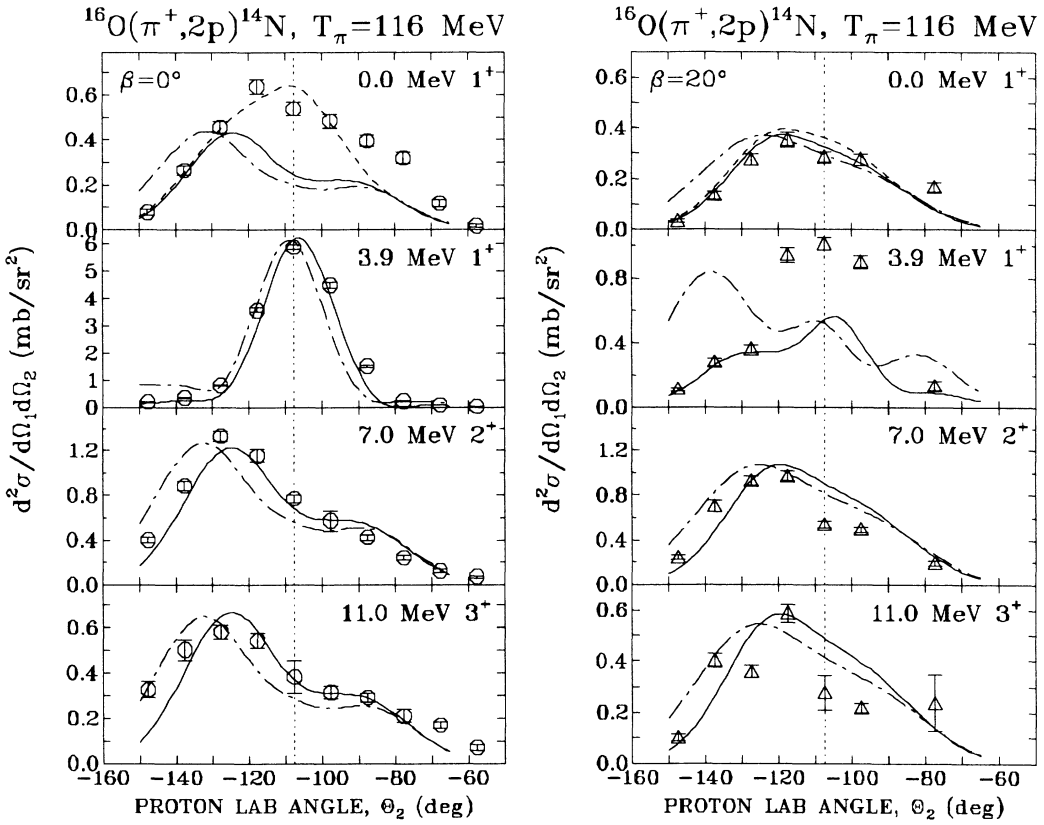

FIG. 3. Proton angular correlations for the strongly excited isoscalar states when the first proton is detected at $\theta_1=+50°$ with respect to the beam. Error bars show the combined statistical and fitting uncertainties. The vertical dotted line indicates the quasifree angle. Results from the in-plane NaI array are labeled $\beta=0°$ while the out-of-plane results are labeled $\beta=20°$. Solid curves are predictions of a factorized DWIA quasi-deuteron model calculation (THREEDEE, Ref. 7), dot-dashed curves are the corresponding PWIA predictions. The calculations have been normalized to the data for each state. Pure $L=0$ angular momentum transfer is used for the 3.9 MeV state (DWIA$\times$7.0), and pure $L=2$ for the 7.0 MeV (DWIA$\times$4.4) and 11.0 MeV (DWIA$\times$1.8) states. The PWIA/DWIA ratio is typically a factor of 6. For the ground state a mixture of $L=2$ and $L=0$ (DWIA$\times$2.3 and 76) (dashed curve) was needed to approximate the shape.

peaked behavior of $L=2$ two-nucleon absorption can be explained by the energy and angle dependence of the elementary (free) $\pi d \rightarrow 2p$ amplitude. First, absorption on a nucleon pair moving away from the pion lowers the effective total energy of the πNN interaction by about 30 MeV (for a 250 MeV/c pair) which, at a beam energy of 116 MeV, lowers the (free) interaction cross section by 30%. These kinematics corresponds to more forward θ_2 lab angles for fixed θ_1. Absorption on a pair moving toward the pion will raise the πNN interaction energy by a similar amount, a region over which the free πd cross section is roughly constant, hence sustaining the backward-angle peak of the correlation. Second, the center-of-mass to laboratory transformation for absorption on a nucleon pair moving towards the pion is smaller than for absorption on a pair at rest, so that reactions detected at fixed θ_1 in the lab arise from smaller center-of-mass angles in the case of a pair moving toward the pion. This case corresponds to larger values for θ_2. Because the free-πd cross section has a $(1+A\cos^2\theta_{\text{c.m.}})$ angular dependence, an effectively larger cross section is seen at more backward θ_2 angles. That the angle and energy dependencies of the free-πd reaction work in the same direction to enhance the observed asymmetries is due to the particular angles and the energy selected for this experiment. The calculation shown in Fig. 3, which reproduces the shape of the $L=2$ angular correlation fairly well, uses these facts to produce the predicted asymmetry of the $L=2$ angular correlation.

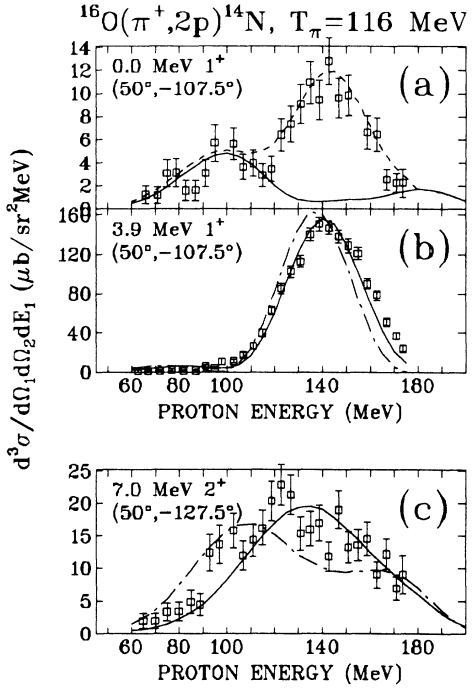

FIG. 4. Energy sharing distributions for the ground state and 3.9 MeV 1^+ states at the quasifree angle pair, and for the 7.0 MeV 2^+ state for 20° away from quasifree. The normalizations for the DWIA and PWIA model calculations are the same as for the previous figure. The double-peaked structure of the ground state indicates the need for a mixture (dashed line) of angular momentum transfer $L=2$ (solid line) and $L=0$. The gap in the ground-state data at about 154 MeV marks the position of the peak of the free $^2H(\pi^+,2p)$ reaction.

The ground-state angular correlation has a shape intermediate between the $L=0$ and $L=2$ shapes exhibited by the other states. The solid line with the ground-state data in Fig. 3 shows the predicted $L=2$ shape, while the long-dashed curve is an *ad hoc* admixture of the $L=0$ shape, ignoring the coherence of the $L=0$ and $L=2$ components. This suggests that two-nucleon pion absorption leading to this state is a mixture of $L=0$ and $L=2$ angular momentum transfer processes, which is in agreement with previous suggestions based on lower energy data[29] and in disagreement with the theoretical spectroscopic factors in Table I. We note that the magnitude of the $L=0$ component is too small to have been identified in the (d,α) measurements of van der Woude and Meijer.[14] In contrast to (d,α), the $(\pi^+,2p)$ reaction permits measurement of zero recoil momentum; therefore our measurements are particularly sensitive to the $L=0$ component. Also, phenomenological wave functions for the ^{14}N ground state obtained by Huffman *et al.*[30] from fitting inelastic-electron-scattering data lead to significantly more $L=0$ strength for the ground state. Their H1 wave function gives an $L=0$ strength which is over twice that needed in the present experiment. Although this wave function does not provide the required suppression of β decay, it is possible that $1s$-$0d$ admixtures contribute to the suppression.[31] In any event uncertainties in the wave function may be sufficient to accommodate the $L=0$ component observed in this experiment. Finally, it may also be that at least part of the effect arises from the tensor polarization effects discussed by Gouweloos and Thies,[19] which are not included in the present calculations. The effective polarization is largest for the $L=2$, $J=1^+$ state.

B. Energy sharing distributions for low-lying $T=0$ states of ^{14}N

The distribution of energy between the two protons for each state is represented by the energy spectrum of one of them. Figures 4(a) and 4(b) show the spectrum of protons, $d^3\sigma/d\Omega_1 d\Omega_2 dE_1$ for the ground state and 3.9 MeV state for the quasifree angle pair.

The 3.9 MeV state is well described by the predicted $L=0$ shape which peaks near the free-πd energy. The DWIA calculation is somewhat better than the PWIA version in predicting the shape, a remark which applies generally to all the results. The ground-state energy sharing distribution is double peaked, as predicted for an $L=2$ transition, but the higher energy peak is centered near 142 MeV, where $L=0$ absorption has a maximum and $L=2$ absorption has a minimum. To separate the $L=0$ and $L=2$ components of absorption leading to the ground state a coherent treatment of the amplitudes is needed. The present framework of the factorized quasi-deuteron calculation can only treat incoherent mixtures of angular momentum transfer $L=0$ and $L=2$. If we assume that the measured cross section is proportional to $\alpha|T_{L=0}|^2+\beta|T_{L=2}|^2$ then we find the experimental

ratio of spectroscopic factors $\alpha/\beta=0.2\pm0.1$. This contradicts the shell-model prediction from Table I of 0.006. This is consistent with the angular correlation data discussed in the previous section.

The energy sharing distribution of the 7.0 MeV $L=2$ state is shown in Fig. 4(c) for (50°, −127.5°) where the angular correlation for this state peaks. (The tail of the strong 3.9 MeV state obscures the 7.0 MeV state at the quasifree angle and prevented extraction of the energy sharing distribution for that setting.) The double humped $L=2$ shape is strongly distorted at this angle in both the data and the calculation.

C. Comparison with the quasi-deuteron DWIA model

The fact that the free $\pi^+ d \rightarrow 2p$ cross section contained in the DWIA model calculation leads to the reproduction of the pronounced asymmetry in the angular distributions for the 2^+ and 3^+ $L=2$ transitions suggests that the $\pi^+ d \rightarrow 2p$ cross section contains much of the important physics of the πNN vertex. The inclusion of initial- and final-state interactions by means of the distorted waves is of relatively minor importance in providing the good description of the shape of the experimental data near quasifree kinematics, as expected from Ref. 7.

On the other hand, we observe that our calculations seriously underpredict the absolute cross sections. This does not necessarily imply serious deficiencies with the basic structure of the reaction model, since several possible explanations of the magnitude discrepancies can be incorporated within the present DWIA calculations. One possible cause is the restriction of the shell-model space to the $0p$ shell. A larger model space leads to additional configurations which may well enhance the cross sections. We note that relatively sophisticated analyses of two-nucleon transfer reactions generally underpredict the absolute cross sections, leading to the inclusion of an overall normalization factor.[32] These problems are much reduced in calculations using an expanded shell-model space.[33]

Another likely source of underestimation of the cross section is the restriction that the relative motion wave function of the *np* pair have the properties of a physical deuteron. Even within the restricted *p* shell space a number of additional states for the *np* pair are allowed. Although the cross sections for $s=0$ pairs and other possible angular momentum states with $l\neq0$ are predicted to be small,[21] their coherent inclusion may enhance the overall cross section. However, in the ^{16}O calculations of Ohta, Thies, and Lee[2] the inclusion of the non-$^3S_1$ pairs leads to only a 20% increase in cross section, insufficient to explain the present discrepancies in magnitude. Possibly more important is our use of the Hulthen radial wave function which effectively makes the (π^+-2N) absorption process long ranged. We would expect a shorter-ranged interaction to enhance the $(\pi^+,2p)$ cross section. To see this we consider a $(0p)^2$ pair coupled to $L=0$ in a harmonic oscillator basis. The transformation to relative and center-of-mass motion leads to two equal $L=0$ amplitudes with center-of-mass motion principal quantum numbers $N=0$ and $N=1$ with corresponding relative motion principal quantum numbers $n=1$ and $n=0$, respectively. The overlap of the relative motion wave function with a Hulthen deuteron wave function projects out primarily the $N=1$ term, whereas the overlap with a short-ranged function would give more comparable contributions from each amplitude. In the extreme limit of a δ-function overlap we would have roughly a factor of 4 enhancement in cross section. Thus one expects a shorter-ranged πNN interaction to lead to significant increases in the $(\pi^+,2p)$ cross section. This possible explanation for at least part of the discrepancy in magnitude is supported by the observation that the discrepancy is largest by almost a factor of 2 for the $L=0$ transitions, compared to $L=2$ which can only have a single amplitude in the $0p$ harmonic-oscillator model. Inclusion of such terms in the DWIA requires a detailed knowledge of the πNN vertex and a removal of the cross section factorization approximation. Efforts in this direction are in progress.

D. Recoil momentum distributions for low-lying $T=0$ states of ^{14}N

In the plane-wave impulse approximation the detected nuclear recoil momentum $\mathbf{p}_R$ is equal and opposite to the momentum of the absorbing nucleon pair. In this section we extract recoil momentum distributions $F(p_R)$ for several states, which for $L=0$ and $L=2$ absorption processes should exhibit characteristic *s*-wave and *d*-wave shapes, respectively. The model used here is separate from the DWIA calculation discussed in the previous sections; it ignores distortions but treats the acceptance of the apparatus fully using a Monte Carlo method. We define the experimentally measured yield $R(\mathbf{p}_R)$ as the un-normalized probability density for pion absorption leading to a given state, and write it as

$$R(\mathbf{p}_R)=|\mathbf{p}_R|^2\int\int T(\mathbf{p}_\pi,\mathbf{p}_R,\mathbf{p}_1,\mathbf{p}_2)a(\mathbf{p}_1,\mathbf{p}_2)\times\delta[\mathbf{p}_\pi+p_R-(\mathbf{p}_1+\mathbf{p}_2)]\times d^3p_1 d^3p_2 \ . \quad (4)$$

Here $T(\mathbf{p}_\pi,\mathbf{p}_R,\mathbf{p}_1,\mathbf{p}_2)$ is the transition matrix element for an interaction leading to a final recoil momentum $\mathbf{p}_R$, with proton momenta $\mathbf{p}_1$ and $\mathbf{p}_2$. The factor $|\mathbf{p}_R|^2$ corresponds to a Fermi gas density of initial two-nucleon states. The acceptance function $a(\mathbf{p}_1,\mathbf{p}_2)$ accounts for the geometrical acceptances and energy cutoffs; in the integration over all possible final states of $\mathbf{p}_1$ and $\mathbf{p}_2$, it takes the value 1 if $\mathbf{p}_1$ and $\mathbf{p}_2$ fall within the acceptance of the apparatus and the value 0 otherwise. The δ function enforces momentum conservation.

Now we make the further assumption that $T(\mathbf{p}_\pi,\mathbf{p}_R,\mathbf{p}_1,\mathbf{p}_2)$ can be factored such that

$$T(\mathbf{p}_\pi,\mathbf{p}_R,\mathbf{p}_1,\mathbf{p}_2)=F(p_R)\times T_{\pi NN}(E'_\pi,\hat{\mathbf{p}}'_1) \ , \quad (5)$$

where $F(p_R)$ depends only on the magnitude of $\mathbf{p}_R$, and represents the recoil momentum distribution which we wish to extract from the data. $T_{\pi NN}(E'_\pi,\hat{\mathbf{p}}'_1)$ is evaluated in the π-two-nucleon center-of-mass frame, which is defined by $\mathbf{p}_R$ and $\mathbf{p}_\pi$, where the effective pion interaction

energy is E'_π, and only the angle of one proton, given by $\hat{\mathbf{p}}'_1$, is relevant. $T_{\pi NN}(E'_\pi,\hat{\mathbf{p}}'_1)$ is unknown, but we have used the energy and angular dependence of the free $\pi d \rightarrow 2p$ cross section. This formulation factors out the forward-backward asymmetry of the angular correlation discussed earlier, since the $\pi d \rightarrow 2p$ cross section is evaluated in the πNN center-of-mass frame. Integrating over the recoil angle Ω_R, the measured recoil momentum distribution $R_0(p_R)\equiv\int R(\mathbf{p}_R)d\Omega$ is then written

$$R_0(p_R)=F(p_R)\,|\,\mathbf{p}_R\,|^2\int\int\int T_{\pi NN}(E'_\pi,p'_1)a(\mathbf{p}_1,\mathbf{p}_2)\times\delta[\mathbf{p}_\pi+\mathbf{p}_R-(\mathbf{p}_1+\mathbf{p}_2)]\times d^3p_1 d^3p_2 d\Omega_R \equiv F(p_R)\times A(\mathbf{p}_R)\,, \tag{6}$$

where $A(\mathbf{p}_R)$ is now the overall acceptance including the energy and recoil angle dependence of the interaction. The evaluation of $F(p_R)$ then follows by dividing $R_0(p_R)$ measured in all detector pairs of the apparatus by the calculated acceptance spectrum $A(\mathbf{p}_R)$. In practice, $A(\mathbf{p}_R)$ was evaluated via a Monte Carlo technique wherein the random variables were $\mathbf{p}_R$, the recoil momentum, and p'_1 the direction of the first proton in the π-quasi-deuteron center-of-mass frame. $T_{\pi NN}(E'_\pi,\hat{\mathbf{p}}'_1)$ was replaced by a weight proportional to the $\pi d \rightarrow 2p$ center-of-mass cross section, given the angle $\hat{\mathbf{p}}'_1$ and the energy E'_π computed for the quasi-deuteron rest frame.

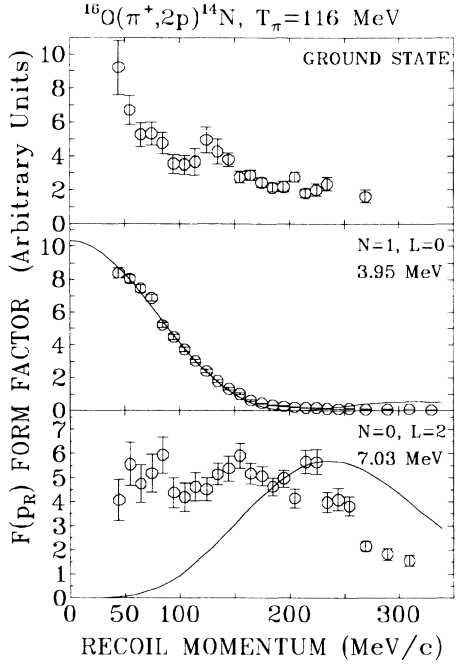

FIG. 5. Recoil momentum distributions for the ground state, 3.9, and 7.0 MeV states averaged over all detectors. In the impulse approximation the measured recoil momentum, p_R is opposite to the momentum of the absorbing np pair. The p_R^2 dependence of a Fermi gas density of states, the p_R energy and angle dependence of the ^{2}H(π^+,2p) reaction, and the kinematical recoil momentum acceptance of the apparatus were calculated and divided out using a Monte Carlo technique (see text). Harmonic-oscillator momentum space probability densities for $L=0$ and 2 are shown for comparison for oscillator parameter 1.17 fm.

$F(p_R)$ is plotted in Fig. 5 for the ground, 3.9 MeV ($L=0$), and 7.0 MeV ($L=2$) states. For comparison, the arbitrarily normalized probability density of harmonic-oscillator states with $N=1$, $L=0$ and $N=0$, $L=2$ are shown. The oscillator parameter is $1.66/\sqrt{2}$ fm, where 1.66 fm is the value derived from elastic electron charge scattering for ^{16}O (Ref. 34), and the factor $\sqrt{2}$ results from the center-of-mass transformation of coordinates for a np pair. The $L=0$ behavior of the 3.9 MeV state is clearly seen, and the chosen harmonic-oscillator probability density reproduces it well. The shape of the distribution agrees with the form factor for this state obtained by Wharton *et al.*[29] at 60 MeV. The data for the 7.0 MeV state exhibit the greater strength at high-recoil momenta expected for an $L=2$ transition relative to the $L=0$ case, but do not fall to zero at low p_R, as does the trivial harmonic-oscillator representation. At low values of p_R there may be some contribution to the spectrum from the neighboring $L=0$ state, but fits to the excitation spectra as a function of p_R showed that this contribution is small. As pointed out by Gouweloos and Thies,[19] the low p_R region in $L=2$ transitions can be filled in by processes such as an admixture of $L=0$ absorption, distortions, or absorption on other than $^3S_1$ pairs. The ground-state data again show behavior intermediate between pure $L=0$ and pure $L=2$ (as approximated by the 7.0 MeV data), in agreement with the earlier data of Wharton *et al.*[29] However, the distinct $L=2$ bump at 180 MeV/c seen by Wharton *et al.* is not seen, but rather a shoulder centered near 140 MeV/c is seen. The resolution of p_R is 50 MeV/c FWHM in this region, possibly washing out some structure. In summary, it appears that the recoil momentum spectra of the three states accessible for this analysis qualitatively confirm the $L=0$, $L=2$, or mixed behavior of absorption leading to them.

E. The integrated (π, 2p) cross section and two-nucleon absorption

In this section we study what the present data imply about the unresolved question of the overall size of the two-nucleon contribution to pion absorption near resonance. The physics interest is to determine whether the two-nucleon absorption dynamics can account for the full absorption cross section, and whether other nonquasifree processes exist in substantial amounts. We have not identified any direct signature in these data of any nonquasifree dynamics, but find that analysis of the excitation energy spectra and angular correlations combined do provide new insights into the strength of the two-nucleon absorption channel.

In order to explore the overall strength of two-nucleon absorption in our data, we have divided it into different regions of excitation of the residual nucleus. Absorption reactions leading to discrete states leave the residual nucleus intact, with no possibility of additional particles in the final state. The three-body continuum begins at 7.6

MeV, so that the proton angular correlation integrated up to this excitation energy is due only to two-body absorption (neglecting multistep processes where additional nucleons are reabsorbed prior to leaving the nucleus). Up to 20 MeV the excitation spectra are dominated by discrete states, and so we may expect this yield to be predominantly from two-nucleon absorption. Above 20 MeV we have rather arbitrarily divided the data into regions bounded by 50, 75, and 100 MeV excitation.

Figure 6 shows the in-plane ($\beta=0$) proton angular correlations for the reaction $^{16}O(\pi^+,2p)^{14}N$ for five excitation energy ranges for $T_\pi=116$ MeV and $\theta_1=50°$. The curves are two-Gaussian fits in which the height, width, and centroids of the peaks were allowed to vary; using these shapes to fit the data is an arbitrary choice, made here to facilitate comparison with other experiments. The data are well represented by the sum of a narrow and a broad Gaussian. For excitation energies up to 7.6 MeV both the narrow and the broad Gaussians result from two-body absorption because this range excludes N-nucleon ($N>2$) final states. In the range up to 20 MeV we expect two-body absorption to dominate the angular correlation but that some three- or four-body final states will also contribute. As the energy range is further raised, many-body final states increasingly contribute, which is reflected by the increasing flatness of the broad component of the angular correlations. We have integrated these fits to the angular correlations over Ω_2 to obtain single differential cross sections $d\sigma/d\Omega_1$. In the horizontal plane our Gaussians are not centered on the quasifree angle, while in the vertical plane, where no angular asymmetry is expected, the Gaussians are centered on $\beta=0$. These results are summarized in Table II. Figure 7 shows the resulting values for $d\sigma/d\Omega_1$ as a function of excitation energy range for the two-component decomposition. We estimate that the energy cutoffs in this experiment (60 MeV $< T_1 <$ 175 MeV, and 30 MeV $< T_2 <$ 200 MeV) have the effect of reducing by up to 50% the measured $(\pi,2p)$ cross section at high excitations where mainly low-energy protons contribute to the data.

The narrow Gaussian component in our fits does not appear to pick out the direct two-nucleon absorption component reliably: For states below 7.6 MeV excitation less than half the cross section is in the narrow Gaussian, although one might assume that these states are purely populated by direct absorption. Figure 7 illustrates the much weaker energy dependence of the narrow-Gaussian component than the broad-Gaussian component. If the cross section in the narrow Gaussian were actually picking out the two-nucleon absorption piece of the angular correlation, it would increase as a function of excitation energy until all of the two-nucleon strength had been included, and then flatten out. The observed behavior is rather the opposite, staying flat in the low-excitation region and then growing slowly.

The present results show that the two-Gaussian decomposition method of analysis is incorrect when ap-

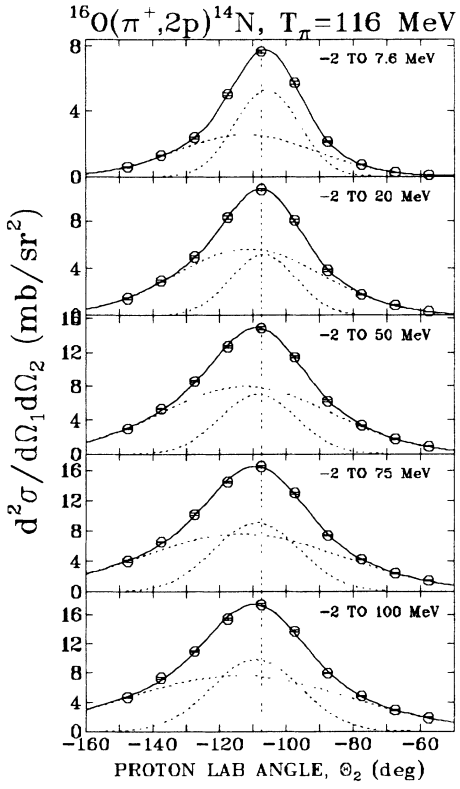

FIG. 6. Proton angular correlations for the reaction $^{16}O(\pi^+,2p)^{14}N$ at $T_\pi=116$ MeV for several ranges of excitation energy when the first proton is detected at 50° with respect to the beam without corrections for events outside the energy acceptance of the apparatus. The fits are two-Gaussian decompositions.

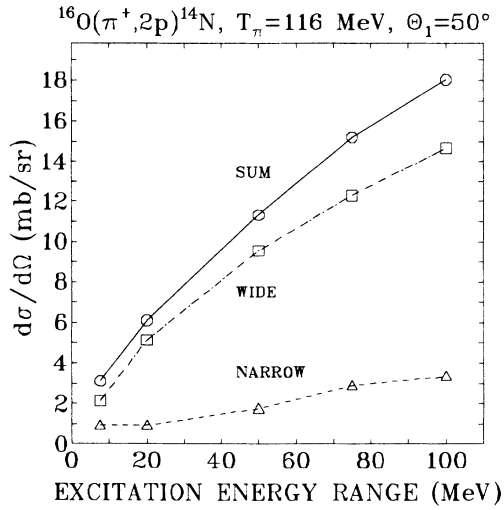

FIG. 7. Single differential cross sections for $^{16}O(\pi^+,2p)^{14}N$ at 116 MeV (solid line) when one proton is detected at 50°, uncorrected for the apparatus' energy acceptance. Dashed and dot-dashed lines correspond to the two-Gaussian decomposition described in the text.

TABLE II. Differential and integrated $^{16}O(\pi^+,2p)^{14}N$ cross sections at 116 MeV for the indicated states and ranges of excitation energy. $d\sigma/d\Omega(50°)$ is the differential cross section for $\theta_1=50°$ in the lab. $\sigma_{tot}(\pi^+,2p)$ is the total two-nucleon cross section extrapolated from 50° (see text). Corrections of up to 20% were applied for the experimental energy acceptance for the highest excitation energy range. Error estimates exclude an overall normalization uncertainty of 10%, as well as the uncertainty in extrapolating the differential cross section at 50° to the total cross section $\sigma_{tot}(\pi^+,2p)$. The value of σ_{abs} was taken from Ref. 35.

E_x (MeV)	$d\sigma/d\Omega(50°)$ (mb/sr)	$\sigma_{tot}(\pi^+,2p)$ (mb)	$\sigma_{tot}/\sigma_{abs}$ (%)
0	0.56±0.06	3.2±0.4	1.6±0.3
3.95	1.7 ±0.1	9.7±0.7	4.7±0.8
7.03	1.2 ±0.1	6.8±0.7	3.3±0.6
11.0	0.8 ±0.1	4.6±0.5	2.3±0.4
−2 to 7.6	3.4 ±0.3	19 ±2	9.4±1.8
−2 to 20.0	6.7 ±0.7	38 ±5	19 ±4
−2 to 50.0	14 ±3	78 ±16	38 ±10

plied to the region of low excitation and discrete states, and that at higher excitations the situation is not at all clear. The contribution from the $L=2$ absorption channels is mainly in the broad Gaussian part of the fit. Only one-third of the $(\pi,2p)$ cross section is included in the narrow-Gaussian component for excitations below the three-nucleon continuum threshold, and one-sixth when the integration limit is 20 MeV, which should still be dominated by two-nucleon absorption. We conclude that the method of two-Gaussian decomposition of angular correlations to extract the direct two-nucleon part of the absorption cross section is not reliable. Since $L>0$ contributions will always widen the angular correlations, the error introduced by using this technique will generally result in an underestimate of the fraction of two-nucleon absorption in the total absorption cross section.

In Fig. 8 we show the proton angular correlations for each of the excitation energy ranges individually, rather than cumulatively as in Fig. 6. The dotted lines are two-Gaussian decompositions, as before. The first two bins, for excitation from −2 to 7.6 MeV and 7.6 to 20 MeV are dominated by absorption leading to discrete states in ^{14}N, as discussed before; note again the asymmetry in the backward direction in the 7.6 to 20-MeV bin, which is a reflection of strong $L=2$ absorption in this energy range.

The most significant point in this figure is that the next bin, from 20 to 50 MeV of excitation, still displays a strong peaking near the quasifree angle, with a width comparable to the 7.6 to 20-MeV bin. This means that there is still a substantial amount of direct 2-N absorption in this energy range. The 53° FWHM of the 20 to 50 MeV distribution also appears to be consistent with this interpretation: If we estimate the Fermi momentum of the emitted nucleon pair according to the nonrelativistic approximation of Altman *et al.*,[3] as $p_{qd}=p_{2p}\times\tan(s)$, where $s=\text{FWHM}/2.36$, we get 150 MeV/c. This is a reasonable expectation for two nucleons in ^{16}O, and equal to that found in Ref. 3. It is not surprising that a significant amount of s-shell and some p-shell absorption strength should lie at excitations of up to about 50 MeV: $(e,e'p)$ data on medium weight nuclei show considerable strength of single-particle states at excitation energies up to 60 MeV in the s shell,[36] while $^{16}O(\pi,\pi p)$ data at 240 MeV also show considerable s-shell removal strength.[37] The last two bins, from 50 to 75 MeV and from 75 to 100 MeV are progressively "flatter," indicating that direct two-nucleon processes have become less important. Our

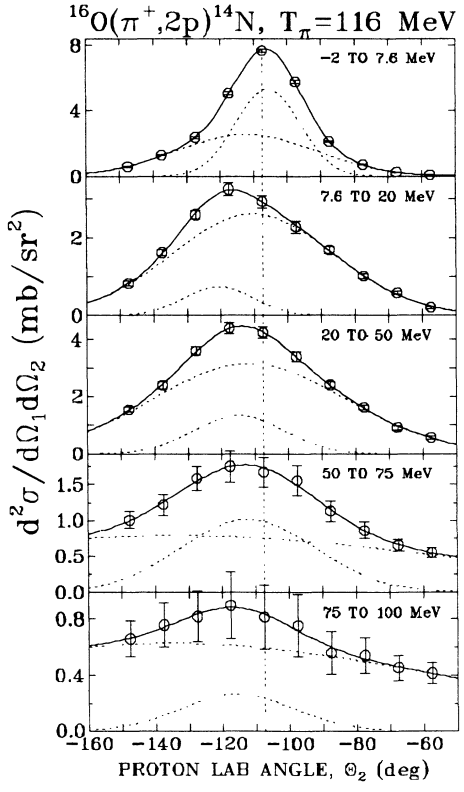

FIG. 8. Proton angular correlations for the reaction $^{16}O(\pi^+,2p)^{14}N$ at $T_\pi=116$ MeV for several ranges of excitation energy when the first proton is detected at 50° with respect to the beam without corrections for events outside the energy acceptance of the apparatus. The fits are two-Gaussian decompositions.

estimates for the fraction of direct two-nucleon pion absorption in the total absorption cross section given in Table II therefore include the energy ranges from -2 to 20 MeV and -2 to 50 MeV. It is obviously difficult to be more quantitative with the data in picking the "best" energy cutoff for extracting the two-nucleon yield. It is probably safe to conclude that the direct two-nucleon cross section lies between the value for the cross section up to 20 MeV excitation and that for the cross section up to 50 MeV excitation.

To estimate the total exclusive $(\pi,2p)$ cross section we must extrapolate $d\sigma/d\Omega_1$ from the present measurement at a single angle θ_1 to all angles. We have assumed that the angular distributions of the states or region in question have the same shape as the $\pi d \rightarrow 2p$ reaction, and multiplied $d\sigma/d\Omega_1$ by the ratio $\sigma_{\pi d}^{\mathrm{TOT}}/(d\sigma/d\Omega)(50°)$, the total absorption cross section to the differential cross section at 50°. Support for the validity of this extrapolation comes from Mack[38] who measured five points of the angular distribution of $^{16}\mathrm{O}(\pi,2p)^{14}\mathrm{N}$ for low excitation energy, and found agreement with the shape of the $^{2}\mathrm{H}(\pi,2p)$ angular distribution. Similar confirmation comes from Arthur *et al.*[39] Its validity for the individual states cannot be tested and remains an *ad hoc* assumption for the present. Table II gives the extrapolated two-nucleon absorption cross sections for the four strongly excited states, and for the regions up to 7.6, 20, and 50 MeV of excitation. One sees that $12\pm1\%$ of the total pion absorption yield in $^{16}\mathrm{O}$ at 116 MeV leads to the four strongly excited states. There must be considerably more two-particle absorption strength in the continuum. Taking the -2 to 20 MeV region as an estimate of a lower limit of the total two-nucleon absorption strength we estimate that at least $19\pm4\%$ of absorption in $^{16}\mathrm{O}$ is found in the two-proton channel. This estimate is about twice as large as that of Altman *et al.*[40] for the case of $^{12}\mathrm{C}$ at 165 MeV. (This factor of 2 difference is also seen in the comparable differential cross section measurements.) The discrepancy could reflect a strong energy dependence; however, we note that the two-Gaussian decomposition may tend to exclude $L>0$ strength from the attributed direct absorption cross section.

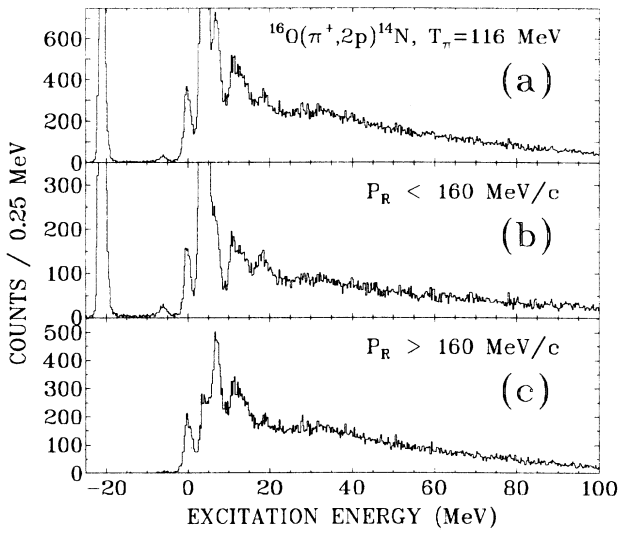

FIG. 9. Excitation energy spectrum of $^{16}\mathrm{O}(\pi^+,2p)^{14}\mathrm{N}$ at $T_\pi=116$ MeV for $\theta_1=50°$, summed over all detectors in the NaI array. With no recoil momentum cut (a), and with limits $p_R<160$ MeV/c (b), and $p_R>160$ MeV/c (c). Peak at -21 MeV is from $^{2}\mathrm{H}(\pi,2p)$ events; counts near -6 MeV are target-holder related background.

Some two-nucleon absorption is not measured directly due to proton final-state scattering which removes events from the angular correlation near quasifree kinematics and low excitation. Calculations of the amount of proton attenuation expected near the present kinematics give factors around 2.5.[19,38] Applying this factor to the 19% of the absorption cross section which we estimate to leave $^{14}\mathrm{N}$ with less than 20 MeV of excitation, we find that some 50% of the total absorption cross section proceeds via the direct quasifree $\pi pn \rightarrow pp$ process. Although some nucleon rescattering processes may leave the nucleus with less than 20 MeV excitation, we note that there is a substantial two-nucleon strength above 20 MeV. Thus, the present results imply that the dominant absorption reaction mechanism in $^{16}\mathrm{O}$ at 116 MeV is two body.

F. Search for deep-lying two-hole states in $^{14}\mathrm{N}$

Deep-lying two-hole states, i.e., states involving the removal of s-shell nucleons, are expected to lie at high excitation energies and to have large widths. Candidates for such states come from a kinematically complete measurement of the $^{16}\mathrm{O}(\pi^-,2n)^{14}\mathrm{N}$ reaction with stopped pions reported by Bassalleck *et al.*[41] Candidate peaks were seen at 18, 31, and 54 MeV excitation energy, of which the latter two were said to agree with the systematics of two-hole state energies estimated from known one-hole states.

Figure 9 shows the $^{16}\mathrm{O}(\pi^+,2p)^{14}\mathrm{N}$ excitation spectrum obtained by summing over all NaI detectors in the array, in order to uncover any broad structures at the higher energies with adequate statistics. The most prominent features of the spectrum are the previously discussed states at 0, 3.9, 7.0, and 11.0 MeV. Figures 9(b) and 9(c) show the effect of the recoil momentum cuts $p_R<160$ MeV/c and $p_R>160$ MeV/c, respectively. The shoulder between 11 and 15 MeV corresponds to several known states which are fairly strong in (d,α) scattering.[14] A bump seen at 18 MeV, seen most clearly in the $p_R<160$ MeV/c spectrum, corresponds to the one seen by Bassalleck *et al.* at this energy. While a very broad shoulder centered near 32 MeV may be discerned, the candidate two-hole state peaks seen in the stopped pion experiment at 31 and 54 MeV are absent. One may speculate that if the peaks seen in the previous experiment are real, then the dynamical differences between the stopped pion and resonance energy pion cases may suppress absorption on the deeper-lying s-shell nucleons in the present experiment.

G. Search for population of $T=1$ states in $^{14}\mathrm{N}$

The strength of pion absorption on nucleon pairs with quantum numbers other than those of the deuteron is of

interest for understanding details of the absorption reaction mechanism. Absorption on $T=1$, $S=0$, $l=0$ pairs cannot happen via an intermediate $N\Delta$ S state, which may suppress $\Delta(1232)$ mechanisms in favor of non-Δ mechanisms.[1,2] Measurements of absorption on such pairs have shown that cross sections for such reactions are 10 to 20 times smaller than on the deuteronlike pairs over a wide range of energies.[21,22] In the present experiment we have looked for population of the $T=1$ state at 2.31 MeV in ^{14}N. This state was included among the degrees of freedom in all fits to the excitation spectra, with the result that it never significantly improved χ^2 [see Fig. 2(b)]. An upper limit of 5% of the $T=0$ strength in the ground state may be assigned to the $T=1$ strength present in the 2.31 MeV state. The two-particle fractional parentage coefficient for coupling to this state is comparable in magnitude to those for the $T=0$ states (see Table I), so this suppression must be of dynamical origin. This ratio between absorption on $T=1$ to $T=0$ pairs is considerably smaller than any reported for total yields; we have measured only one forward proton angle, however, so we cannot rule out the possibility that the ratio is reduced by differing angular distributions for the two transitions.

Other weakly excited states were required in fits to some excitation spectra. Between 3.9 and 7.0 MeV a state was needed near the quasifree geometry; no states with a simple structure are found in this energy region. At other angle settings between 7 and 11 MeV, some strength was needed in the fits for good χ^2 which may belong to two known $T=1$ states in this region, but may also result from continuum excitation or target related background.

V. THE ^{18}O(π^+,2p)^{16}N REACTION

Altman *et al.*[40] measured the direct (π^+,2p) cross section on ^{18}O (extracted from the inclusive angular correlations) at 165 MeV to be 1.05±0.03 times that on ^{16}O, compared to a measured total absorption cross section ratio of 1.17±0.05. The relative smallness of the former ratio was interpreted as a possible sign of dynamical suppression of absorption on nucleon pairs in different shells. In the present experiment we have measured the reaction ^{18}O(π^+,2p)^{16}N with good energy resolution in an attempt to explore the role of cross shell absorption. ^{16}N has a group of four closely spaced states below 0.4 MeV which have particle-hole structure [either $(p_{1/2}^{-1}d_{5/2})$ or $(p_{1/2}^{-1}s_{1/2})$] (Ref. 42) which should be populated by absorption on nucleon pairs in different shells. There is then a gap in excitation energy of 3.0 MeV, followed by a dense spectrum of states, of which many are strongly populated in (d,α) reactions. The complexity of the energy level spectrum indicates that core polarization effects are important, and that not all "cross-shell" absorption states are to be found in the low-lying cluster. Nevertheless, our measurement is the first to resolve the low-lying cluster in the (π^+,2p) reaction in this energy range, explicitly identifying a cross-shell channel.

Figure 10 contrasts the excitation energy spectra for the reactions on the two isotopes for three angle pairs

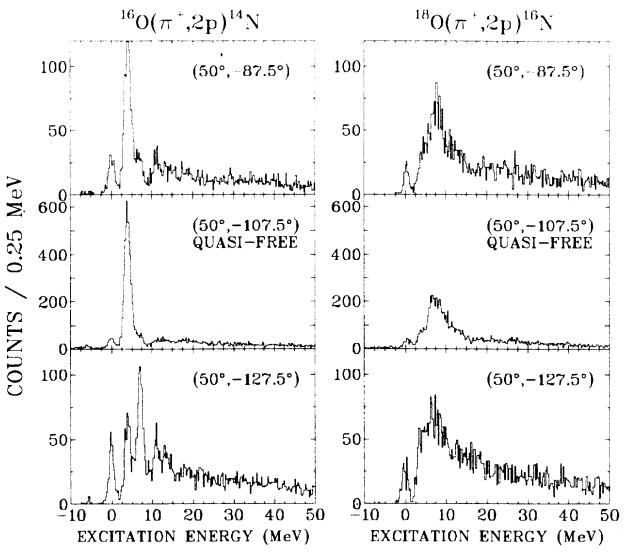

FIG. 10. Comparison of the excitation spectra of ^{16}O(π^+,2p)^{14}N and ^{18}O(π^+,2p)^{16}N for $T_\pi=116$ MeV at three angle pairs (θ_1,θ_2). The vertical axes are normalized with respect to each other (Ref. 43). The peak at 0 MeV in the ^{18}O case is a cluster of four unresolved states.

close to quasifree kinematics. The scales can be compared directly.[43] In the ^{18}O case one sees the group of low-lying states which represent absorption on a valence neutron and a p-shell proton, and a general lack of other prominent states. Only a shoulder near 4 MeV is seen, which probably corresponds to the 3.36 MeV 1^+, 3.5 MeV 2^+ and 3.96 MeV 3^+ states, and a peak in the midst of a cluster of states near 7.5 MeV. Treating these data as in the ^{16}O case, the angular correlation of the low-lying cluster is shown in Fig. 11(a), together with the angular correlations for the first 20 MeV [Fig. 11(b)] and 100 MeV [Fig. 11(c)] of excitation. Integrating these angular correlations to get $d\sigma/d\Omega_1$ we find 0.36±0.02 mb/sr in the low-lying cluster, and 5.9±0.4 mb/sr in the first 20 MeV of excitation including the low-lying cluster. (The normalization uncertainty of 10% is not included in these errors.) Thus 6.1±0.6% of two-nucleon pion absorption at this kinematics involves the valence nucleons of ^{18}O. This is a lower bound since some "cross-shell" states sit not in the low-lying cluster but in the higher-lying regions of the spectra.

The relative normalization error between the two targets in this experiment makes useful quantitative comparison of the ^{18}O and ^{16}O results difficult. The ratio of single differential cross sections in the excitation energy range −2 to 100 MeV is 1.13±0.13, compatible with unity and with the ratio of Altman *et al.* for the total (π^+,2p) cross sections at 165 MeV. The yields from ^{18}O up to 20 MeV excitation is 0.8±0.08 mb/sr less than that from ^{16}O, but there is a sensitivity of about 0.25 mb/sr per 1 MeV change in the excitation energy cut. It is not clear how one can define an equivalent excitation energy cut for the two reactions: For example absorption on two-core nucleons leads to states of at least 3.5 MeV exci-

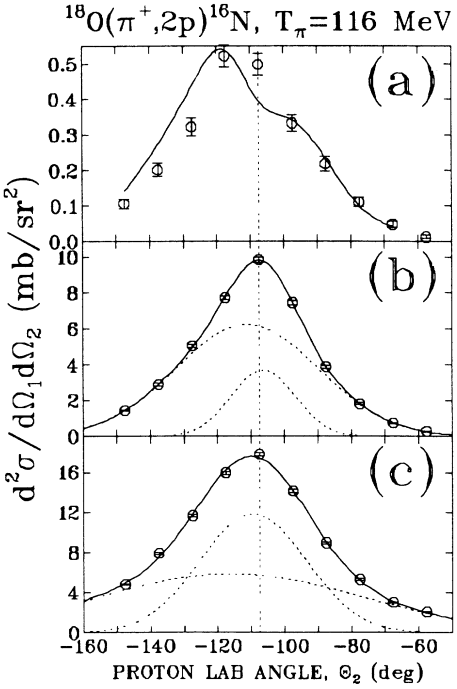

FIG. 11. Proton angular correlations for $^{18}O(\pi^+,2p)^{16}N$ at $T_\pi=116$ MeV for $\theta_1=50°$, and for (a) the ground-state cluster, (b) the excitation energy range -2 to 20 MeV, and (c) the range -2 to 100 MeV. The vertical dotted line indicates the quasifree angle. The curve (a) is a DWIA calculation using the same model as in Fig. 3, while the curves (b) and (c) are two-Gaussian fits to the data.

tation in ^{16}N. The ratio of the yield up to 20 MeV excitation to that up to 100 MeV excitation is 0.37 ± 0.04 for ^{16}O, and 0.29 ± 0.03 for ^{18}O. The ratio of these latter two ratios, which is not affected by the relative normalization uncertainty is 0.78 ± 0.11, although raising the 20 MeV cut in ^{16}N by 3 MeV would raise this to 0.88. This may imply a lower fraction of the two nucleon yield at lower excitation energies for ^{18}O; expected additional rescattering in the ^{18}O reaction would presumably give an effect in this direction.

The possible suppression of absorption on nucleons from different orbitals can only be evaluated in the context of some model of the absorption process. We have estimated the contribution from the two additional neutrons by calculating the parentage for $^3S_1$ pairs using the microscopic model discussed in Sec. II, using a harmonic-oscillator shell-model basis to describe ^{18}O. Specifically, the ground-state wave function was assumed to be a closed ^{16}O core with the additional two neutrons described by a mixture of $(0d_{5/2})^2$, $(1s_{1/2})^2$, and $(0d_{3/2})^2$ configurations with amplitudes 0.927, 0.224, and 0.300, respectively. These amplitudes were estimated from the single nucleon pickup relative spectroscopic factors obtained in the $^{18}O(p,d)^{17}O$ studies of Pignanelli *et al.*[44] The ^{16}N final states were obtained by coupling a $1s$ or $0d$ neutron to a $0p_{1/2}$ or $0p_{3/2}$ proton hole. Projecting out the $^3S_1$ pairs with zero oscillator quanta of relative motion and assuming that Q-value effects are small, we obtain the quasi-deuteron spectroscopic factors listed in Table III. These correspond simply to the normalizations obtained by integrating the function $|\phi_{L\Lambda}(\mathbf{r})|^2$ over all space. The use of pure final-state configurations introduces little error, since configuration mixing in typical shell-model calculations for these states is small.[45]

Assuming that the integrals over the angular correlations carried out to extract $d\sigma/d\Omega$ cover essentially the full yield for all L values, we expect the cross sections to be proportional to the sum of these spectroscopic factors. Inspection of Table III clearly leads one to expect a relatively small yield to the ground-state quartet when compared to the $(0p)^{-2}$ positive parity states present in the first 20 MeV or so of excitation. In fact, for the pure configurations the expected yield is less than 6% of that for $(0p)^{-2}$ states.

As a more refined estimate of the expected yield, we have carried out DWIA calculations for the ground-state quartet following the above assumptions. The resultant calculations for the angular correlation are shown in Fig. 11(a) normalized to the experimental data. The required normalization factor is 6.7, which is within the range of values obtained for $(0p)^2$ transitions. We expect the inclusion of configuration mixing in the ^{16}N states to reduce this value somewhat. Thus, we find no evidence for dynamical suppression of pion absorption on nucleon pairs from different orbitals beyond that expected on the basis of a two-nucleon mechanism involving $^3S_1$ pairs.

VI. SUMMARY AND CONCLUSIONS

We have studied the reactions $^{16}O(\pi^+,2p)^{14}N$ and $^{18}O(\pi^+,2p)^{16}N$ with good energy resolution at 116 MeV for θ_1 fixed at 50° and for a wide range of θ_2 centered on the quasifree angle. Restricting the reaction to low excitation and near-quasi-free kinematics allows us to see and

TABLE III. Quasi-deuteron spectroscopic factors S_d for absorption leading to the given shell-model configurations in the reaction $^{18}O(\pi^+,2p)^{16}N$

Configuration	J^π	L	S_d	Sum
Ground-state quartet				
$(1s_{1/2},0p_{1/2}^{-1})$	$0^-,1^-,2^-$	1	0.15	
$(0d_{5/2},0p_{1/2}^{-1})$	$2^-,3^-$	3	0.35	0.5
p-shell core				
$(0p)^{-2}$	$0^+,1^+$	0	1.50	
	$1^+,2^+,3^+$	2	7.50	9.0

study the effects of nuclear structure on the two-body pion absorption mechanism. We conclude that we have found evidence of pion absorption leading to two-nucleon final states which can be described by angular momentum transfer $L=0$ and 2 in a p-shell nucleus. Proton angular correlations, energy sharing distributions, and recoil momentum distributions for several low-lying states in ^{14}N support this. A factorized quasi-deuteron DWIA calculation confronted with these data can successfully describe the shapes but not the magnitudes of some of the measured distributions; several reasons are given for the discrepancies. Absorption leading to the ground state is more complex than expected based on Cohen-Kurath nuclear structure predictions.

The behavior of the integrated angular correlations, and the shapes of the angular correlations for low-excitation regions show that the two-Gaussian decomposition method of extracting the two-body component of pion absorption is unreliable. Previous estimates of the two-body absorption component under a variety of conditions may be too small. We estimate that at 116 MeV close to 20% of the absorption cross section leads to the emission of two protons and low excitation of the residual system when integrating up to 20 MeV of excitation. Furthermore, significant two-nucleon absorption strength is shown to exist at higher excitation, though it is difficult to quantify. This means that at 116 MeV the two-body mechanism is dominant after one accounts for initial- and final-state interactions.

We find no evidence for narrow high-lying two-hole states corresponding to absorption on *ss* or *sp* nucleon pairs, which is at variance with results from a stopped pion experiment. Absorption to the $T=1$ isospin partner of the ground state at 2.3 MeV is weak; we set an upper limit of 5% relative to the ground state, which may be the best such limit obtained so far on a medium-weight nucleus.

Finally, "cross-shell" absorption leading to the low-lying group of states in the ^{18}O(π^+,2p)^{16}N reaction was isolated for the first time. At least 6% of direct two-body absorption (as defined by a 20 MeV cut on excitation) in this nucleus involves the valence neutrons, showing that cross shell absorption is not prohibited. No evidence was found for unexpected dynamical suppression of absorption on nucleon pairs from different orbitals.

ACKNOWLEDGMENTS

We thank W. J. Burger, M. Botje, S. Gutzwiller, and D. Renker for assistance during data taking. This work was supported in part by the U.S. National Science Foundation and the Department of Energy.

*Present address: Department of Physics, Carnegie Mellon University, Pittsburgh, PA 15213.
†Formerly the Swiss Institute for Nuclear Research.
‡Present address: Department of Physics, University of Manchester, Manchester M13 9PL, England.
§Present address: TRIUMF, Vancouver B.C., Canada.
**Present address: Department of Physics, University of Pennsylvania, Philadelphia, PA 19104.

[1]Daniel Ashery and John P. Schiffer, Annu. Rev. Nucl. Part. Sci. **36**, 207 (1986).
[2]K. Ohta, M. Thies, and T.-S.H. Lee, Ann. Phys. (N.Y.) **163**, 420 (1985).
[3]A. Altman *et al.*, Phys. Rev. Lett. **50**, 1187 (1983); Phys. Rev. C **34**, 1757 (1986).
[4]W. J. Burger *et al.*, Phys. Rev. Lett. **57**, 58 (1986).
[5]E. Bellotti, D. Cavalli, and C. Matteuzzi, Nuovo Cimento **18A**, 75 (1973); J. Favier *et al.*, Nucl. Phys. **169A**, 540 (1971).
[6]B. G. Ritchie, N. S. Chant, and P. G. Roos, Phys. Rev. C **30**, 969 (1984). See also D. Ashery, Phys. Rev. C **32**, 333 (1985); B. G. Ritchie, N. S. Chant, and P. G. Roos, *ibid.* **32**, 334 (1985).
[7]P. G. Roos, L. Rees, and N. S. Chant, Phys. Rev. C **24**, 2647 (1981); N. S. Chant, computer code THREEDEE (unpublished).
[8]W. R. Gibbs and W. B. Kaufmann, in AIP Conf. Proc. **163**, 279 (1988).
[9]R. D. McKeown *et al.*, Phys. Rev. C **24**, 211 (1981).
[10]R. Tacik, E. T. Boschitz, W. Gyles, W. List, and C. R. Ottermann, Phys. Rev. C **32**, 1335 (1985).
[11]W. Brückner *et al.* Nucl. Phys. **A469**, 617 (1987).
[12]G. Backenstoss *et al.*, Phys. Rev. Lett. **55**, 2782 (1985).
[13]V. Girija and D. S. Koltun, Phys. Rev. Lett. **52**, 1397 (1984).
[14]A. van der Woude and R. J. Meijer, Nucl. Phys. **A258**, 199 (1976).
[15]S. Cohen and D. Kurath, Nucl. Phys. **A141**, 145 (1970).
[16]J. F. Amann *et al.*, Phys. Rev. C **23**, 1635 (1981).
[17]A. Nadasen *et al.*, Phys. Rev. C **23**, 1023 (1981).
[18]L. R. B. Elton and A. Swift, Nucl. Phys. **A94**, 52 (1967).
[19]M. Gouweloos and M. Thies, Phys. Rev. C **35**, 631 (1987).
[20]N. S. Chant *et al.* (to be published).
[21]K. A. Aniol *et al.*, Phys. Rev. C **33**, 1714 (1986).
[22]G. Backenstoss *et al.*, Phys. Lett. B **137**, 329 (1984).
[23]J. P. Albanese *et al.*, Nucl. Instrum. Methods **158**, 363 (1979); 1981 SIN Users Handbook.
[24]J. P. Albanese *et al.*, Nucl. Phys. **A350**, 301 (1980).
[25]J. B. Walker and G. A. Rebka, Jr., Los Alamos Report No. LA-7731-MS, 1979 (unpublished).
[26]B. G. Ritchie *et al.*, Phys. Rev. C **27**, 1685 (1983).
[27]S. Wood, MIT doctoral thesis, 1983 (unpublished).
[28]*TRIUMF Kinematics Handbook,* edited by D. F. Measday, M. R. Menard, and J. E. Spuller.
[29]W. R. Wharton *et al.*, Phys. Rev. C **31**, 526 (1985).
[30]R. L. Huffman, J. Dubach, R. S. Hicks, and M. A. Plum, Phys. Rev. C **35**, 1 (1987).
[31]S. Cohen and D. Kurath, Nucl. Phys. **73**, 1 (1965).
[32]B. F. Bayman and D. H. Feng, Nucl. Phys. **A205**, 513 (1973).
[33]D. H. Feng *et al.*, Phys. Rev. Lett. **44**, 1037 (1980).
[34]C. W. DeJager, H. DeVries, and C. DeVries, At. Nucl. Data Tables **14**, 479 (1974). The proton form factor was factored out in the quoted number.
[35]C. H. Q. Ingram *et al.*, Phys. Rev. C **27**, 1578 (1983).
[36]J. Mougey *et al.*, Nucl. Phys. **A262**, 461 (1976).
[37]G. S. Kyle *et al.*, Phys. Rev. Lett. **52**, 974 (1984).
[38]D. J. Mack, University of Maryland doctoral thesis, 1987 (unpublished); D. J. Mack *et al.* (to be published).
[39]E. D. Arthur *et al.*, Phys. Rev. C **11**, 332 (1975).

[40]A. Altman *et al.*, Phys. Lett. B **144**, 337 (1984); Phys. Rev. C **34**, 1757 (1986).
[41]B. Bassalleck *et al.*, Nucl. Phys. **A343**, 365 (1980).
[42]P. V. Hewka, C. H. Holbrow, and R. Middleton, Nucl. Phys. **88**, 561 (1966).
[43]The ^{18}O data have been renormalized by a factor of 1.45 to make the scales comparable. To convert the vertical axes to the cross section $d^3\sigma/d\Omega_1 d\Omega_2 dE_x$ [mb/sr^2/(0.25 MeV)], divide by 782.
[44]M. Pignanelli, J. Gosset, F. Resmini, B. Mayer, and J. L. Escudie, Phys. Rev. C **8**, 2120 (1973).
[45]J. Millener, private communication.